Published in final edited form as:
Am J Physiol Heart Circ Physiol. 2007 December ; 293(6): H3379–H3387. doi:10.1152/ajpheart.00967.2007.

The visceral pericardium: macromolecular structure and contribution to passive mechanical properties of the left ventricle

Paul D. Jöbsis, **Hiroshi Ashikaga**, **Han Wen**, **Emily C. Rothstein**, **Keith A. Horvath**, **Elliot R. McVeigh**, and **Robert S. Balaban**
Laboratory of Cardiac Energetics, National Heart, Lung, and Blood Institute, National Institutes of Health, Bethesda, Maryland

Abstract

Much attention has been focused on the passive mechanical properties of the myocardium, which determines left ventricular (LV) diastolic mechanics, but the significance of the visceral pericardium (VP) has not been extensively studied. A unique en face three-dimensional volumetric view of the porcine VP was obtained using two-photon excitation fluorescence to detect elastin and backscattered second harmonic generation to detect collagen, in addition to standard light microscopy with histological staining. Below a layer of mesothelial cells, collagen and elastin fibers, extending several millimeters, form several distinct layers. The configuration of the collagen and elastin layers as well as the location of the VP at the epicardium providing a geometric advantage led to the hypothesis that VP mechanical properties play a role in the residual stress and passive stiffness of the heart. The removal of the VP by blunt dissection from porcine LV slices changed the opening angle from 53.3 ± 10.3 to 27.3 ± 5.7° (means ± SD, $P < 0.05$, $n = 4$). In four porcine hearts where the VP was surgically disrupted, a significant decrease in opening angle was found (35.5 ± 4.0°) as well as a rightward shift in the ex vivo pressure-volume relationship before and after disruption and a decrease in LV passive stiffness at lower LV volumes ($P < 0.05$). These data demonstrate the significant and previously unreported role that the VP plays in the residual stress and passive stiffness of the heart. Alterations in this layer may occur in various disease states that effect diastolic function.

Keywords

collagen; diastolic function; myocardial elasticity; residual stress; water permeability; elastin; 2-photon microscopy; porcine heart; optical properties

Diastolic mechanics of the left ventricle (LV) are a result of dynamic interactions of filling pressure (39), mitral valve mechanics (17), and LV wall properties (4). The mechanical properties of the LV wall, resulting from a variety of cellular and extracellular elements, determine active relaxation and passive stiffness of the LV during diastole (7,41). The passive mechanical elements of the entire myocardium have been extensively studied (10,15,18). Another mechanical element that is separate from the LV wall is the encasing parietal pericardium (PP). The PP influences right ventricle (RV) and LV interactions and limits the ventricular volume as well as influences the overall the pressure-volume relationship of the heart, in vivo (29,31,35). Despite the fact that the visceral pericardium (VP) shares many physical aspects of the PP (18), including a closed structure that completely encompasses the

Address for reprint requests and other correspondence: R. S. Balaban, National Heart, Lung, and Blood Institute, National Institutes of Health, Bldg. 10, Rm. B1D416, MSC 1061, 9000 Rockville Pike, Bethesda, MD 20892 (rsb@nih.gov)..

myocardium and similar composition, the mechanical impact of the VP to the overall myocardium has largely been neglected.

Found in all vertebrates, the VP is also known as the cardiac epimysium. This outermost layer of the epicardium consists of a thin layer of mesothelial cells over a dense network of collagen and elastin fibers. The VP surrounds the myocardium, securing the coronary vasculature, and acts as a barrier between cardiomyocytes and the pericardial fluid. Unlike the endocardium, this connective tissue develops embryologically from extracardiac tissue known as the proepicardial serosa (20). The tensile strength and stiffness of the VP is significantly greater than that of other myocardial tissues(26); however, its macromoleular structure and impact on LV diastolic mechanics have not previously been reported.

In this study, we examined the configuration and function of the VP to test the hypothesis that it contributes significantly to the passive mechanical property of the LV. To characterize the VP structure, fluorescence and two-photon second harmonic excitation microscopy was used to generate en face three-dimensional volumetric images of the porcine VP. This approach permitted a novel view of the macromolecular microstructure of the VP. The impact of the VP on the passive mechanical properties of the LV was determined from the opening angle and pressure-volume relationships in vitro.

MATERIALS AND METHODS

Following a protocol approved by the National Heart, Lung, and Blood Institute Institutional Animal Care and Use Committee, 10 domestic Yorkshire pigs (5 male and 5 female; weight: 45–60 kg) were initially anesthetized with an intramuscular injection of atropine (0.01 mg/lb), xylazine (1.0 mg/lb), ketamine HCl (3 mg/lb), and butorphanol (0.1 mg/lb) followed by securing venous access through the ear vein and subsequent intubation for transport. In the operating room, animals were mechanically ventilated and anesthetized with 1.5–2% isoflurane balanced with medical oxygen and air to achieve ~60% O_2 in the inspired gas. The chest was opened through a midline sternotomy. The PP was opened and fashioned into a cradle to support the heart. Potassium chloride (4 meq/kg) was administered intravenously to induce asystole, and the heart was quickly excised.

Opening angle measurements

In four pigs immediately following induced asystole, the heart was removed, rinsed with saline, and cut equatorially to obtain three 1-cm-thick cross-sectional slices of the LV. Midventricular slices were obtained, avoiding the mitral valve and apex of the heart. The RV free wall was removed from each slice close to the septal wall, leaving the LV intact. All three LV slices were kept in saline while the VP was removed from one of the slices at room temperature. The majority of this layer could be peeled away using blunt dissection with forceps. The VP was separated from myocytes with minimal damage to myocytes of the myocardium as judged by direct inspection with both fluorescence and histological staining (see Fig. 1, *A* and *B*). From this dissection, the extensive connectivity of this structure was directly observed with elastic fibers running millimeters over the surface of the heart. Once removed, the VP of ~1 cm^2 was compressed down to a small white mass of ~2 mm in diameter, attesting to the elastic nature of this material. Each LV slice was floated in saline and photographed before and after a radial transmural cut was made in the LV free wall, following previously published protocols (23). The opening angle of a LV slice was defined as the angle between the two radial lines connecting the center of the ventricular chamber and the centerlines of the walls at the cut edges. LV slices with intact and removed VP were photographed (Nikon D1x with 60-mm Micro Nikkor lens) at approximately the same time to avoid any difference in residual stress due to differences in time-dependent factors. The elapsed time from excision of the heart to photographing the opening angle was <30 min.

Microscopic examination and optical characterization

For two-photon excitation microscopy, small fresh tissue samples (<1 cm^3) were collected from LV slices by dissection. Micrograph images were typically collected as a series of *x*-*y* planes as a function of tissue depth (so-called "*z* stack") from the outer VP surface to myocytes and from the endocardial surface to myocytes using an inverted Zeiss LSM510 NLO META microscope. The META 32 element detector was calibrated using methods described in Jobsis et al. (14). Typically, fluorescence and second harmonic emissions were simultaneously acquired by the META multielement PMT detector and two-photon excitation at 786 nm. Collection of the fluorescence emission of elastin using four or five of the META's 11-nm-wide elements centered at elastin's peak emission wavelength (468 nm) and the backscattered second harmonic generation (B-SHG) from collagen on the META's 393-nm centered element (Figs. 2 and 3) allowed simultaneou collection of collagen and elastin images through all but the thickest samples of the VP. In thicker samples, fluorescence and B-SHG were collected sequentially using the microscope's more sensitive nondescanned detector with a 465-nm centered (50-nm full width at half-maximum) bandpass filter by varying the excitation from 710 nm for elastin and NADH fluorescence and 920 nm to induce B-SHG emission from collagen. Fluorescence and harmonic images were collected in the same setting, providing an accurate registration of the interwoven pattern found in elastin and collagen. The distinctive spectral differences of elastin's two-photon-induced fluorescence and collagen's second harmonic generation (primarily by type I) have been described (8,38,42) and allowed classification of these extracellular fibers. To provide further conformation of collagen and elastin found with two-photon techniques, light micrographs of fixed tissue were performed using Movat's staining techniques (21).

Determination of the elastin, collagen, and epicardial myocyte orientation in relation to the LV of the intact heart was done on three intact hearts. Alignment of the heart along an axis from the apex (i.e., apical dimple) to the left aortic valve commissure between mitral valvular annulus and the aorta provided the *z*-axis analogous to Streeter et al.'s classic fiber orientation study (36). Using the Zeiss microscope with an Olympus ×20 objective on an objective inverter (LSM Technologies, www.lsmtech.com) with a PIFOC P-725 objective *z*-drive (Physik Instrumente, www.physikinstrumente.com) allowed the collection of images demonstrating the fiber orientation on the intact heart (30). To facilitate fiber image collection from multiple locations with precision, longitudinal and transverse strips of the epicardium (~40 × 10 × 4 mm) were imaged in several locations using the ×40 Zeiss lens with the standard microscope stage configuration. The use of two-photon excitation fluorescent microscopy allowed imaging of the full thickness of the VP in most locations. Collagen and elastin fiber orientation was measured from the surface of the VP to the VP-myocardium interface, including the first layer of myocytes at various locations on the ventral surface of the LV. Sampling locations formed an inverted "L" starting near the apex (see Fig. 4 for a diagram of the locations).

Pressure-volume measurements

To estimate the effects of the VP on passive mechanical properties of the intact heart, we needed to develop an approach that would disrupt the mechanical coupling of the VP across the heart. It was determined to be impractical to peel the VP off of the intact heart; thus, we used a surgical approach of cross-hatching the VP across the entire LV. Using this approach, it was impossible to perform this procedure in vivo or in the perfused heart in vitro due to unavoidable damage to the large surface vessels located just under the VP. To perform this task, the hearts of four pigs were arrested and quickly excised from the animal, rinsed, and placed in warm (35–39° C) saline. A catheter with a compliant latex balloon (condom) was placed in the LV retrograde across the aortic valve and secured in place. The mitral valve was clamped and monitored during the study to ensure that it remained closed. In the absence of the heart, no pressure was recorded using the volumes applied in this study. Ten-milliliter aliquots of saline were instilled

into the balloon, and catheter pressure was recorded via an inline pressure transducer. The full range of the pressure-volume relationship was recorded three times. The heart was then removed from saline, and the VP was disrupted using a modified no.11 surgical blade with a mechanical stop that exposed only 300–400 μm of the blade tip. Shallow incisions were made in a parallel cross-hatched pattern with incision lines ~3–5 mm apart over the entire exposed free wall of the LV. The heart was quickly returned to warm saline, and the pressure-volume relationship measurement was repeated three times. All pressure-volume relationship measurements were completed in <45 min. The effectiveness of the surgical VP disruption was confirmed by measuring the opening angle of LV slices with surgically disrupted VPs. Chamber stiffness [change in pressure over volume (dP/dV)] was calculated between each increment in volume from the acquired ex vivo pressure-volume relationship measurements described above. Two additional animals were used as controls to determine the effect of time on the pressure-volume relationship to ensure that the effects seen after the disruption of the VP were not due to unrelated changes in myocardial stiffness due to postmortem contractions.

Statistical analysis

Values are presented as means ± SD unless otherwise specified. A paired *t*-test was used to compare pressure-volume relationships. Single-factor ANOVA and two-factor repeated-measures ANOVA, followed by a Tukey test (40), were used to evaluate opening angles and the effect of VP disruption and added volume on LV passive stiffness. Statistical tests were performed using Microsoft Excel 2002, and statistical significance was accepted at $P < 0.05$.

RESULTS

Microscopic examination

Movat-stained micrographs of cross sections of fixed VP demonstrated the pattern and abundance of collagen (yellow) and elastin (black) layers in the VP, as shown in Fig. 1. The VP was easily distinguished from myocytes of the epicardium and did not appear to infiltrate the myocardium but instead formed a distinct layer covering the myocytes, consistent with the ease of dissection (Fig. 1*B*). The VP varied in thickness from 40 to >200 μm and was typically thicker near the apex and vessels of the heart. The collagen density appeared to be much greater in the VP than anywhere in the myocardial wall. Images of the VP by two-photon excitation microscopy at three different depths taken from *z*-stack series are shown in Fig. 2. (Movie renderings of a typical *z*-stack through the VP are shown in Supplemental Movie 1.)[1] These images were acquired from the surface of the VP down to ~50-μm depth. Elastin, detected by its intrinsic fluorescence, is shown in Fig. 2, *A–C*, whereas collagen in the same image plane, detected by its B-SHG, is shown in Fig. 2, *D–F*. In general, elastin structures were dispersed fibrous cords running across the entire field of view. In contrast, collagen was densely packed with the characteristic sinusoidal fiber pattern with a period of 10–15 μm under these conditions. At the outer surface of the VP (Fig. 2, *A* and *D*), elastin was deposited in parallel rods running with collagen diagonally around the heart. The average orientation of collagen and elastin on the ventral wall of the LV was −33.8 ± 12.2° at the surface of the VP (Fig. 4). At the midlevel (Fig. 2, *B* and *E*), elastin structures became a more complex network unrelated to the orientation of collagen, which became more variable at this level. In many samples, the orientation of collagen showed a slight rotation; however, distinct collagen bundles apparently unrelated to surface collagen orientation were also found. At the VP-myocyte interface (Fig. 2, *C* and *F*), the parallel structure of elastin and collagen returned again to be aligned with the long axis of collagen fibers. Myocyte orientation was found to be 73 ± 16° on the ventral surface of the LV myocardium with elastin and collagen again aligned parallel to each other and nearly

[1]Supplemental material for this article is available online at the American Journal of Physiology-Heart and Circulatory Physiology website.

perpendicular to the myocyte orientation. Near blood vessels, subsurface collagen and elastin orientation appeared to be dominated by that of the vessel structure, although at the surface and myocyte-VP interface, collagen and elastin were similar to other areas.

Two-photon excitation microscopic and Movat-stained micrograph images from the endocardium revealed a different pattern (Figs. 1*C* and 3, *A*–*F*). Endocardial surface images showed both elastin and collagen layers to be more diffuse and disorganized. The elastin content was extensive, although individual elastin rods appeared less substantial than those found in the VP. In both imaging methods used, there appeared to be less collagen distributed throughout the endocardial layer. Several layers of elastin were observed overlaying the layer of Purkinje cells and a single layer separating these cells from myocytes. We were typically able to image deeper into the myocardium (~100 μm) from the endocardial side of the LV, which was likely due to a reduction in primary tissue scattering of the excitation beam by the reduced collagen content.

Opening angles

Opening angles were 53.3 ± 10.3° in intact LV slices, 27.4 ± 5.7° in slices with peeled VP, and 35.5 ± 4.0° in slices with surgically disrupted VP (Fig. 5, *A*–*C*). Myocardial slices with either peeled or disrupted VP showed significantly different opening angles than slices with intact VP ($P < 0.05$ by ANOVA and Tukey test). It was also interesting to note that tissue blocks with an intact VP used for two-photon microscopy had a strong tendency to curl, forming a concaved epicardial surface that essentially flattened with the removal of the VP. This observation is also consistent with the VP contributing to the opening angle and playing a major role in passive mechanical properties of the myocardium. Opening angles of LV slices from hearts with surgically disrupted VP were not significantly greater than those of slices with removed VP, indicating that the surgical approach mechanically uncoupled the VP. However, it is unlikely that the surgical disruption of the VP is as effective as the peeling of the VP in reducing the opening angle due to substantial epicardial areas with attached VP.

Pressure-volume relationships

Disruption of the VP resulted in a significant decrease, or rightward shift, of the pressure-volume relationship (Fig. 6). Although the pressure-volume relationship with either intact or disrupted VP was highly reproducible within an individual animal, it was variable between animals, likely due to differences in heart size. The VP disruption resulted in a significant decrease in the passive stiffness of the LV at lower volumes (Fig. 7). However, there were no significant differences in the passive stiffness between intact and disrupted VPs at higher volumes. No time-dependent pressure-volume behavior was detected in the three sequential experiments conducted during control and VP-disrupted conditions. In control animals, no significant changes in the pressure-volume relationship were seen during the first 60 min. Dramatic and unmistakable left shifts in the pressure-volume relationship were seen after ~80 min due to postmortem contraction. Once myocardial rigor began, the changes in the pressure-volume relationship were rapid, with a threefold increase in the pressure-volume relationship at 90 min. This increase in pressure was most pronounced at higher LV volumes. No similar changes in the pressure-volume relationship were seen in experiments that were completed well before the postmortem contraction began.

DISCUSSION

The hypothesis that the VP contributes significantly to LV passive mechanical properties was primarily derived from our gross dissection experience and is supported by our observations of its microscopic three-dimensional composition and configuration as well as its location at the geometrically advantageous outer edge of the heart. Experimental results supported this

hypothesis. First, the opening angle of the LV slices, which reflects the level of myocardial residual stress, was highly dependent on the presence of the VP. Second, mechanical uncoupling of the VP in the intact heart led to a modest rightward shift of the pressure-volume relationship and a decrease in LV passive stiffness at lower volumes. Based on these results, we conclude that the VP plays a significant role in the passive mechanical properties of the LV in early diastolic filling.

Several previous lines of evidence support the role of the VP in the passive mechanical properties of the heart. The VP tensile strength is more than an order of magnitude greater than that of any other portion of the myocardium, which agrees with the greater hydroxyproline content found in this layer (26). In addition, the epicardium with the VP has greater stiffness than the intact endocardium (16,26).

The VP may also have a role in storing elastic energy during systole and releasing it in early diastole to aid the relaxation and untwisting of the LV. In human hearts, the systolic deformation of the epicardial surface is characterized by a longitudinal shortening of 10% (37), shear due to ventricular twisting of 20° from the base to apex (19), and a small amount circumferential shortening. Although direct measurements of circumferential shortening of the epicardial surface are not available, geometric considerations and direct myocardial measurements have shown a decrease of circumferential strain from endocardial to epicardial layers and the strain on the epicardial surface is likely low by the trend of these measurements (2,3). Using these typical values and assuming that they are uniform over most of the epicardial surface, we calculated the composite deformation of the epicardial surface and the associated shortening or stretching of a segment of elastin fiber at a range of fiber angles from −90 to 90°. We modeled the two cases of no appreciable circumferential shortening and 2% shortening. The result is shown in Fig. 8. Indeed, given the measured fiber angles in this study (Fig. 4), the elastin fibers should be stretched during systole. The resulting elastic return force should actively contribute to the relaxation and untwisting of the LV. The epicardial location of the VP is again advantageous in two aspects: the circumferential shortening is minimum and, correspondingly, the elastin fiber lengthening is maximum; the torque from the elastic recoil is also maximized. The epicardial location of the VP also permits this function with minimal impact on the contractile apparatus within the wall by not being interleaved with the contractile elements. The VP can also serve as a final safety factor limiting the expansion of the heart beyond critical limits due to its tensile strength. Clinical cases of near-myocardial rupture resulting from acute myocardial infarction have been documented (12), where the myocardium had separated and only the VP remained resisting the ventricular pressure, also attesting to the VP tensile strength and its ability to provide a final barrier to myocardial rupture.

It is of note that that the VP has a very low hydraulic water permeability (L_p) as well as low diffusional water permeability (1). In addition, the pressure gradient at the surface of the heart has been estimated to be very steep (32), suggesting that the very low filtration coefficient of the VP may also prevent plasma filtration across the heart wall into the pericardial sack. No “solid” macromolecular structure, such as the elastic lamina in arterial walls, was observed in the VP. Thus, the low L_p is likely due to the extensive tight junctions in the endothelial layer (13) and not a function of the macromolecular structure.

Although the opening angle may not be a complete description of the residual stress, it does reflect the overall level of residual stress in the myocardium (24). The opening angle is a measure of two-dimensional residual strain, which quantifies the circumferential deformation of the LV slice when the residual stress is relieved. A zero opening angle indicates no residual stress, and the angle positively correlates with the residual stress (23). The primary source of residual stress has been considered to arise from deformation of cellular (e.g., titin) (4,6,11) and extracellular elements (e.g., perimysial collagen fibers along myofibers) (5,27) within the

myocardium from the stress-free state to the unloaded state (28). However, our results clearly demonstrate that the VP has a significant impact on the opening angle and, therefore, must make a major contribution to the residual stress of the LV. The increased opening angles found in epicardial portions of myocardium slices are consistent with the VP being an important factor in the residual stress found in the resting heart (24). This concept is also supported by the report by Omens et al. (25), which showed that the opening angle does not change during pressure overload despite significant cardiomyocyte hypertrophy. We speculate that earlier studies of the opening angle in physiological and pathological states may have been confounded by modifications of the VP that need to be accounted for beyond the changes within the myocardium itself. For example, the stiffness of the VP increases within the infarcted region of the myocardium during an acute period after myocardial infarction associated with small changes in total hydroxyproline content (26). Alterations in the VP composition and structure could play a role in numerous pathological states associated with passive mechanical properties that warrant further investigation.

In the intact heart, we found that mechanically uncoupling the VP only modestly decreased the passive stiffness of the LV at lower volumes, with no effect at higher volumes (Fig. 7). In comparison, the PP has been shown to impact many mechanical aspects of the myocardium, including the diastolic pressure-volume curve as well as RV-LV contraction interactions (33). Since we were unable to work with a contracting myocardium, we could only compare the diastolic pressure-volume effect of the PP with our data on the VP disruption. In addition, no study on the role of the PP in the porcine heart is available, which is of some concern since the structure and mechanics of the PP are species dependent (22). Data on PP removal are primarily from canines and somewhat quantitatively variable depending on the laboratory and experimental methods. In an early study by Spotnitz and Kaiser (34) on in vitro canine hearts, the ventricle stiffness [dP/dV (in mmHg/ml)] was 0.98 in control and 0.67 without the pericardium over very modest increases in ventricular volumes (from 0 to ~18 ml) and pressures (from ~0 to 15 mmHg), representing a 46% decrease in stiffness with the removal of the PP. This effect in the in vitro canine heart was comparable with what was observed at low volumes with the removal of the VP, which also decreased the stiffness by ~50% (see Fig. 7). However, the removal of the PP has been shown to dramatically reduce the stiffness of the myocardium at very high volumes in numerous studies (9,29,31), which was not observed in this study (see Figs. 6 and 7). This comparison implies that the VP is important in the elastic component of the myocardium, as indicated by the effects at low ventricular volumes, its dramatic compression on dissection, and the impact on opening angle of the myocardial slices, but has little impact on the limitation of ventricular volume compared with the myocardium itself or the PP in vivo. Currently, no information is available on the role of the encasing VP on the LV and RV pressure interactions that have been well characterized as a consequence of an intact PP (9,29,33).

The endocardium was compared with the structure of the VP using two-photon excitation and classical histological approaches. Due to the highly irregular surface of the endocardium and its location, we did not attempt to strip this layer in our opening angle experiments or mechanically uncouple it in the intact heart experiments. However, the structures of the two layers were similar with more elastin and less collagen found in the endocardial layers (see Figs. 1–3), consistent with the more extensive opening angles found with endocardial sections than with epicardial sections by Omens et al. (24), which we confirmed in this study (data not shown). Thus, the endocardial layer of elastin may also contribute to the net residual strain of the myocardium; however, we were not able to confirm this directly due to the inability to dissect this layer free from the wall.

The optical properties of the VP present some interesting challenges for using a variety of optical techniques to examine the intact heart. The strong fluorescence of VP elastin

significantly interferes with the detection of NAD(P)H or any blue fluorescence from the surface of the heart using conventional one-photon excitation schemes. The spectral emission of the elastin is also essentially identical to tissue NAD(P)H fluorescence (Fig. 9), providing no spectral analysis solution. The strong UV absorbance of the VP acts as a very significant primary filter that severely limits the penetration of UV light to myocytes in confocal experiments on extracted tissues blocks (Fig. 9*B*). With regard to two-photon excitation, we suggest that the scattering properties of collagen severely disrupted the point-spread function of the infrared light as a function of depth through the VP. This notion was supported by measurements of transmission characteristics of the dissected VP that revealed a strong light-scattering spectrum (Fig. 9*B*). In, addition we found that we could consistently optically penetrate to the myocytes from the endocardial surface but less frequently from the epicardial surface, which was consistent with the relative collagen content of these two structures. Thus, the scattering and emission properties of the VP will generate significant problems with regard to obtaining optical signals from cardiac myocytes, in vivo.

In conclusion, the microstructures of macromolecules of the endocardium and epicardium have been determined. The VP was found to significantly contribute to the residual strain of the myocardium but not impact overall passive properties of the intact myocardium to the same extent as the PP. The VP apparently has its largest effect on elastic components of the heart at low ventricular volumes, or early diastole. We suggest that the composition and mechanical properties of the VP should be considered in mechanical models of myocardium function and, more importantly, in a variety of clinical conditions with demonstrated alterations in diastolic function that might be reflecting changes in this diminutive structure.

Supplementary Material

Refer to Web version on PubMed Central for supplementary material.

Acknowledgments

The authors gratefully acknowledge the assistance and technical support of Joni Taylor, Kathy Lucas, Katie Hope, Michael Nauman, and William Schenke.

REFERENCES

1. Agostoni E, Bodega F, Zocchi L. Equivalent radius of paracellular “pores” of the mesothelium. J Appl Physiol 1999;87:538–544. [PubMed: 10444610]
2. Aletras AH, Balaban RS, Wen H. High-resolution strain analysis of the human heart with fast-DENSE. J Magn Reson 1999;140:41–57. [PubMed: 10479548]
3. Aletras AH, Wen H. Mixed echo train acquisition displacement encoding with stimulated echoes: an optimized DENSE method for in vivo functional imaging of the human heart. Magn Reson Med 2001;46:523–534. [PubMed: 11550245]
4. Bell SP, Nyland L, Tischler MD, McNabb M, Granzier H, LeWinter MM. Alterations in the determinants of diastolic suction during pacing tachycardia. Circ Res 2000;87:235–240. [PubMed: 10926875]
5. Burlew BS, Weber KT. Connective tissue and the heart. Functional significance and regulatory mechanisms. Cardiol Clin 2000;18:435–442. [PubMed: 10986582]
6. Cazorla O, Freiburg A, Helmes M, Centner T, McNabb M, Wu Y, Trombitas K, Labeit S, Granzier H. Differential expression of cardiac titin isoforms and modulation of cellular stiffness. Circ Res 2000;86:59–67. [PubMed: 10625306]
7. Covell JW. Factors influencing diastolic function. Possible role of the extracellular matrix. Circulation 1990;81:III155–III158. [PubMed: 2297881]
8. Cox G, Kable E, Jones A, Fraser I, Manconi F, Gorrell MD. 3-Dimensional imaging of collagen using second harmonic generation. J Struct Biol 2003;141:53–62. [PubMed: 12576020]

9. Glantz SA, Misbach GA, Moores WY, Mathey DG, Lekven J, Stowe DF, Parmley WW, Tyberg JV. The pericardium substantially affects the left ventricular diastolic pressure-volume relationship in the dog. Circ Res 1978;42:433–441. [PubMed: 624151]
10. Granzier HL, Irving TC. Passive tension in cardiac muscle: contribution of collagen, titin, microtubules, and intermediate filaments. Biophys J 1995;68:1027–1044. [PubMed: 7756523]
11. Helmes M, Trombitas K, Granzier H. Titin develops restoring force in rat cardiac myocytes. Circ Res 1996;79:619–626. [PubMed: 8781495]
12. Helmy TA, Nicholson WJ, Lick S, Uretsky BF. Contained myocardial rupture: a variant linking complete and incomplete rupture. Heart 2005;91:e13. [PubMed: 15657203]
13. Ishihara T, Ferrans VJ, Jones M, Boyce SW, Kawanami O, Roberts WC. Histologic and ultrastructural features of normal human parietal pericardium. Am J Cardiol 1980;46:744–753. [PubMed: 7435384]
14. Jobsis PD, Combs CA, Balaban RS. Two-photon excitation fluorescence pH detection using 2,3-dicyanohydroquinone: a spectral ratiometric approach. J Microsc 2005;217:260–264. [PubMed: 15725129]
15. Kang T, Humphrey JD, Yin FC. Comparison of biaxial mechanical properties of excised endocardium and epicardium. Am J Physiol Heart Circ Physiol 1996;270:H2169–H2176.
16. Kang T, Yin FC. The need to account for residual strains and composite nature of heart wall in mechanical analyses. Am J Physiol Heart Circ Physiol 1996;271:H947–H961.
17. Karlsson MO, Glasson JR, Bolger AF, Daughters GT, Komeda M, Foppiano LE, Miller DC, Ingels NB Jr. Mitral valve opening in the ovine heart. Am J Physiol Heart Circ Physiol 1998;274:H552–H563.
18. Kluge T, Hovig T. The ultrastructure of human and rat pericardium. I. Parietal and visceral mesothelium. Acta Pathol Microbiol Scand 1967;71:529–546. [PubMed: 4869325]
19. Lorenz CH, Pastorek JS, Bundy JM. Delineation of normal human left ventricular twist throughout systole by tagged cine magnetic resonance imaging. J Cardiovasc Magn Reson 2000;2:97–108. [PubMed: 11545133]
20. Manner J, Perez-Pomares JM, Macias D, Munoz-Chapuli R. The origin, formation and developmental significance of the epicardium: a review. Cells Tissues Organs 2001;169:89–103. [PubMed: 11399849]
21. Movat HZ. Demonstration of all connective tissue elements in a single section; pentachrome stains. AMA Arch Pathol 1955;60:289–295. [PubMed: 13248341]
22. Naimark WA, Lee JM, Limeback H, Cheung DT. Correlation of structure and viscoelastic propoerties in the pericardia of four mammalian species. Am J Physiol Heart Circ Physiol 1992;263:H1095–H1106.
23. Omens JH, Fung YC. Residual strain in rat left ventricle. Circ Res 1990;66:37–45. [PubMed: 2295143]
24. Omens JH, McCulloch AD, Criscione JC. Complex distributions of residual stress and strain in the mouse left ventricle: experimental and theoretical models. Biomech Model Mechanobiol 2003;1:267–277. [PubMed: 14586695]
25. Omens JH, Rodriguez EK, McCulloch AD. Transmural changes in stress-free myocyte morphology during pressure overload hypertrophy in the rat. J Mol Cell Cardiol 1996;28:1975–1983. [PubMed: 8899556]
26. Przyklenk K, Connelly CM, McLaughlin RJ, Kloner RA, Apstein CS. Effect of myocyte necrosis on strength, strain, and stiffness of isolated myocardial strips. Am Heart J 1987;114:1349–1359. [PubMed: 3687688]
27. Robinson TF, Cohen-Gould L, Factor SM, Eghbali M, Blumenfeld OO. Structure and function of connective tissue in cardiac muscle: collagen types I and III in endomysial struts and pericellular fibers. Scanning Microsc 1988;2:1005–1015. [PubMed: 3399840]
28. Rodriguez EK, Omens JH, Waldman LK, McCulloch AD. Effect of residual stress on transmural sarcomere length distributions in rat left ventricle. Am J Physiol Heart Circ Physiol 1993;264:H1048–H1056.
29. Ross J Jr. Acute displacement of the diastolic pressure-volume curve of the left ventricle: role of the pericardium and the right ventricle. Circulation 1979;59:32–37. [PubMed: 758121]

30. Rothstein EC, Nauman M, Chesnick S, Balaban RS. Multi-photon excitation microscopy in intact animals. J Microsc 2006;222:58–64. [PubMed: 16734715]
31. Shabetai R, Mangiardi L, Bhargava V, Ross J, Higgins CB. The pericardium and cardiac function. Prog Cardiovasc Dis 1979;22:107–134. [PubMed: 384458]
32. Smith NP. A computational study of the interaction between coronary blood flow and myocardial mechanics. Physiol Meas 2004;25:863–877. [PubMed: 15382827]
33. Spodick, DH. The Pericardium: a Comprehensive Textbook. Dekker; New York: 1997.
34. Spotnitz HM, Kaiser GA. The effect of the pericardium on pressure-volume relations in the canine left ventricle. J Surg Res 1971;11:375–380.
35. Stokland O, Miller MM, Lekven J, Ilebekk A. The significance of the intact pericardium for cardiac performance in the dog. Circ Res 1980;47:27–32. [PubMed: 7379265]
36. Streeter DD Jr, Spotnitz HM, Patel DP, Ross J Jr, Sonnenblick EH. Fiber orientation in the canine left ventricle during diastole and systole. Circ Res 1969;24:339–347. [PubMed: 5766515]
37. Wen H, Bennett E, Epstein N, Plehn J. Magnetic resonance imaging assessment of myocardial elastic modulus and viscosity using displacement imaging and phase-contrast velocity mapping. Magn Reson Med 2005;54:538–548. [PubMed: 16086299]
38. Williams RM, Zipfel WR, Webb WW. Interpreting second-harmonic generation images of collagen I fibrils. Biophys J 2005;88:1377–1386. [PubMed: 15533922]
39. Yellin EL, Meisner JS. Physiology of diastolic function and transmitral pressure-flow relations. Cardiol Clin 2000;18:411–433. vii. [PubMed: 10986581]
40. Zar, JH. Biostatistical Analysis. Prentice Hall; Upper Saddle River, NJ: 1998.
41. Zile MR, Brutsaert DL. New concepts in diastolic dysfunction and diastolic heart failure: part I: diagnosis, prognosis, and measurements of diastolic function. Circulation 2002;105:1387–1393. [PubMed: 11901053]
42. Zipfel WR, Williams RM, Christie R, Nikitin AY, Hyman BT, Webb WW. Live tissue intrinsic emission microscopy using multiphoton-excited native fluorescence and second harmonic generation. Proc Natl Acad Sci USA 2003;100:7075–7080. [PubMed: 12756303]

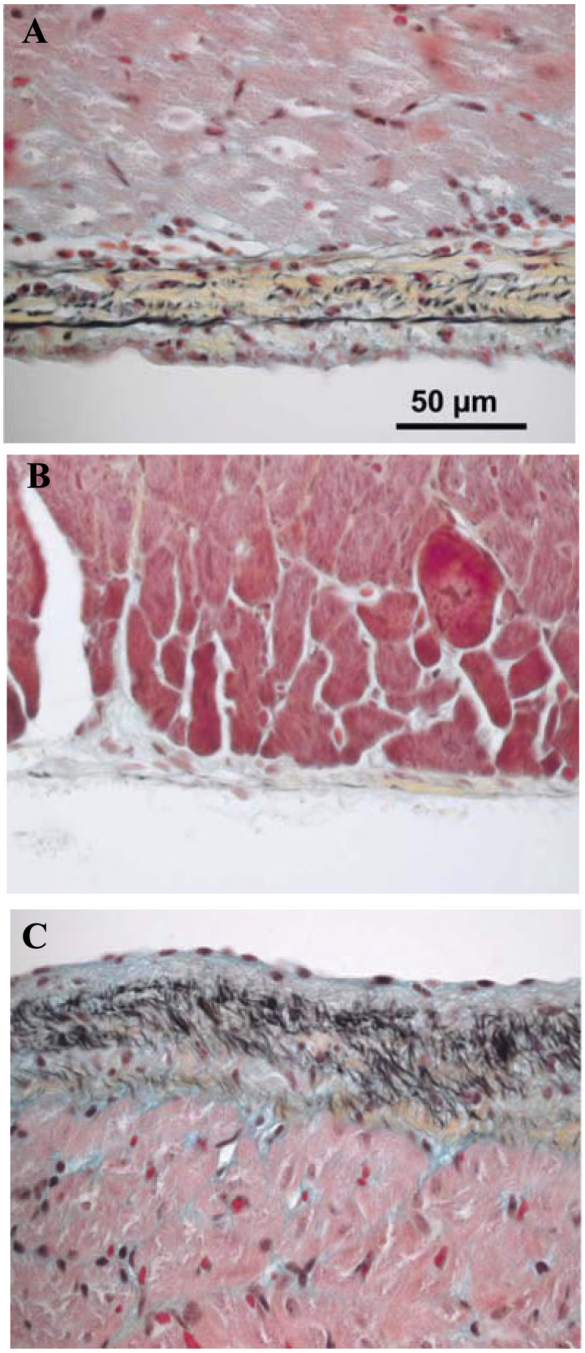

Fig. 1.

Micrographs of cardiac tissue with Movat staining. Collagen appears gold, and elastin fibers appear dark purple or black. The intact visceral pericardium (VP; *A*) appears to consist primarily of collagen with distinct layers of elastin fibers. Following blunt dissection, the VP is almost completely removed (*B*). The intact endocardial membrane (*C*) appears to be rich in elastin relative to the collagen density. The 50-μm scale bar in *A* applies to all images.

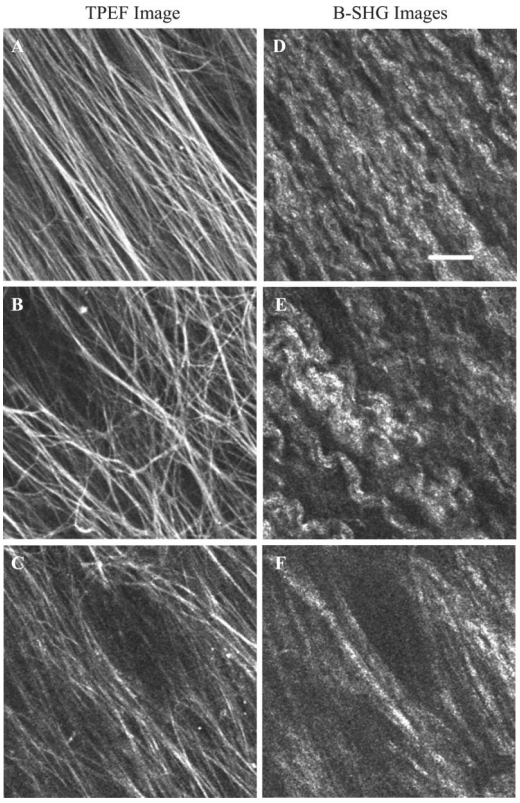

Fig. 2.

Two-photon excitation fluorescence (TPEF) and backscattered second harmonic generation (B-SHG) micrographs of a relatively thin area of VP collected simultaneously using a Zeiss LSM 510 META microscope. At the surface (8 μm) of the VP, parallel elastin rods (*A*) run along the long axis of collagen fibers (*D*). In the midsection of the VP (16 μm), elastin rods (*B*) form a network that appears to be independent of collagen orientation (*E*). At the VP and myocyte interface (30 μm), elastin rods (*C*) again appear to follow the orientation of collagen fibers (*F*). This pattern was found in most VP samples imaged in this manner, although the pattern was interrupted by blood vessels within the VP. The scale bar in *D* represents 20 μm and applies to all images.

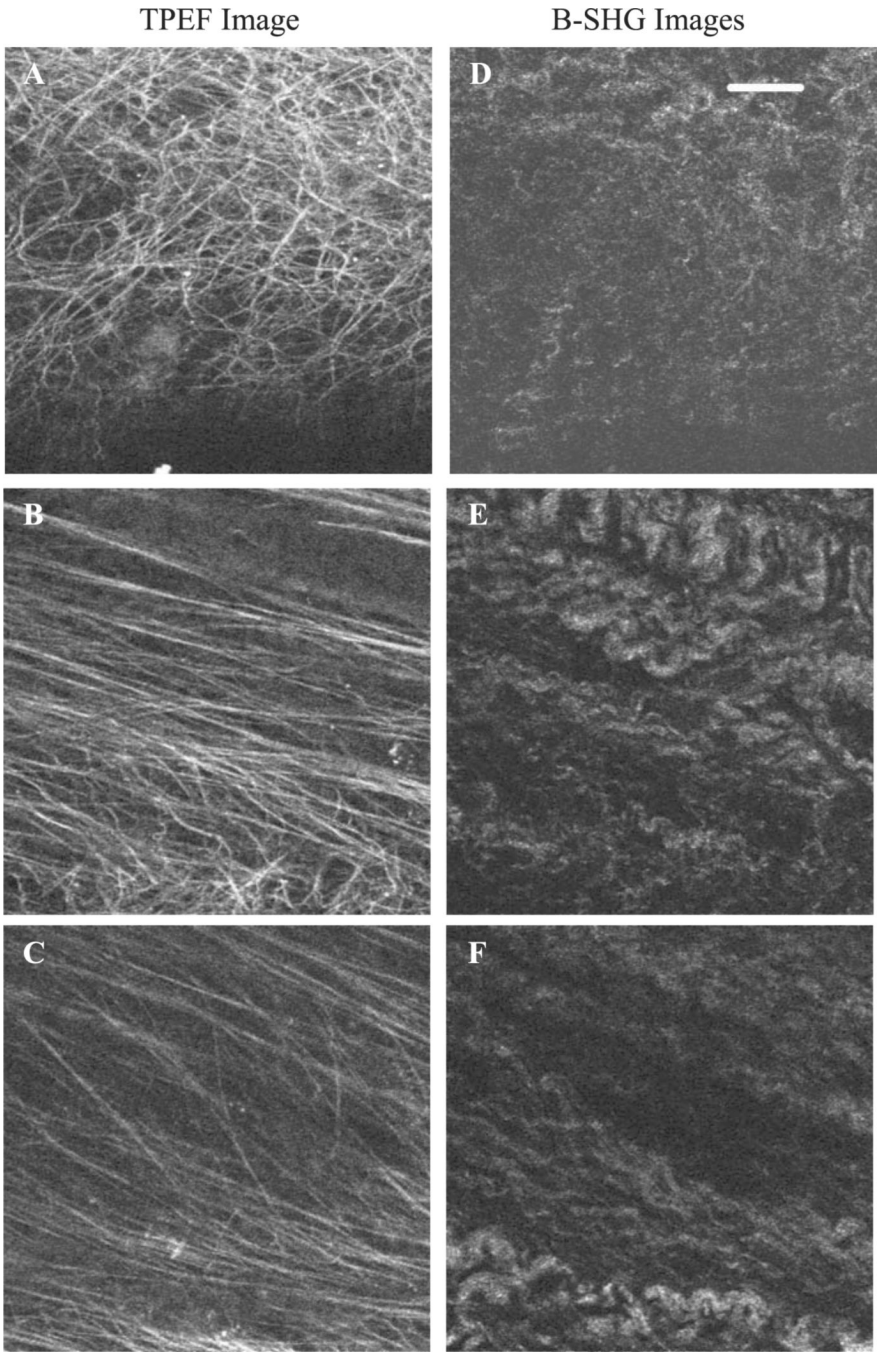

Fig. 3.

TPEF and B-SHG micrographs of a thin section of endocardial membrane. Images show the endocardial membrane at depths of 4 μm (*A* and *D*), 15 μm (*B* and *E*), and 30 μm (*C* and *F*). The endocardial membrane has a similar pattern of collagen and elastin, but the elastin and collagen appear thinner and more diffuse and do not follow the patterns found in the VP. Imaging parameters, laser power, and filter settings were identical to those used in Fig. 2. The scale bar in *D* represents 20 μm and applies to all images.

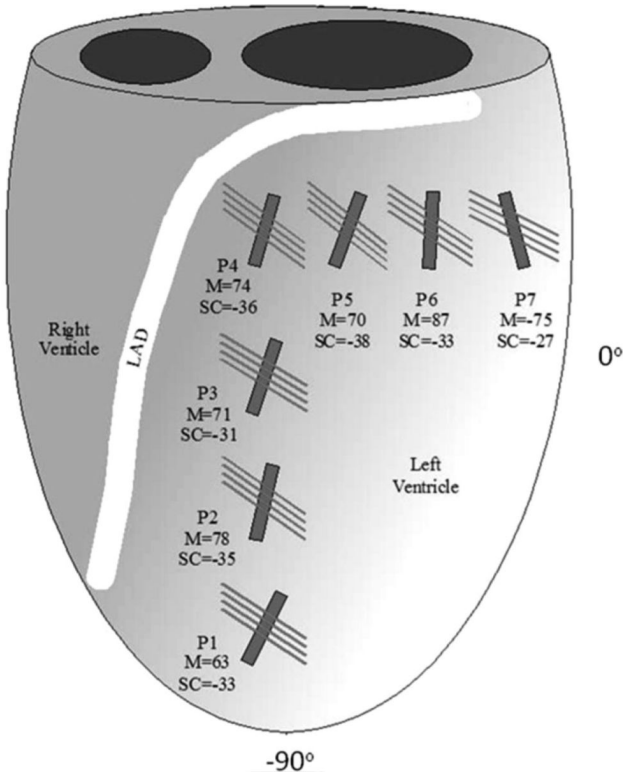

Fig. 4.

Diagram of the left ventricle (LV) and right ventricle showing the imaging locations [*positions 1–7* (P1–P7)] for the fiber orientation survey. LAD, left anterior descending coronary artery. Surface collagen and elastin (SC) of the VP run parallel to each other and are represented by the long narrow lines. The shorter and thicker solid lines represent the average myocyte (M) orientation from the VP-myocardium interface. The surface collagen and elastin orientation and VP-myocardium interface myocyte orientation (means ± SD, $n = 4$) are as follows: P1, −34 ± 9° and 63 ± 3°; P2, −35 ± 21° and 78 ± 3°; P3, −31 ± 8° and 71 ± 1°; P4, −36 ± 14° and 74 ± 9°; P5, −38 ± 12° and 70 ± 23°; P6, −34 ± 12° and 87 ± 43°; and P7, −27 ± 10° and −75 ± 7°.

Fig. 5.

Representative photographs of the opening angle of LV slices with intact (*A*), peeled (*B*), and disrupted VPs (*C*), respectively. ANOVA and Tukey analysis of the opening angles showed that the average opening angle ($n = 4$) for LV slices with either peeled (27.4 ± 5.7°) or disrupted VP (35.5 ± 4.0°) had significantly ($P < 0.05$) reduced opening angles compared with LV slices with an intact VP (53.3 ± 10.3°).

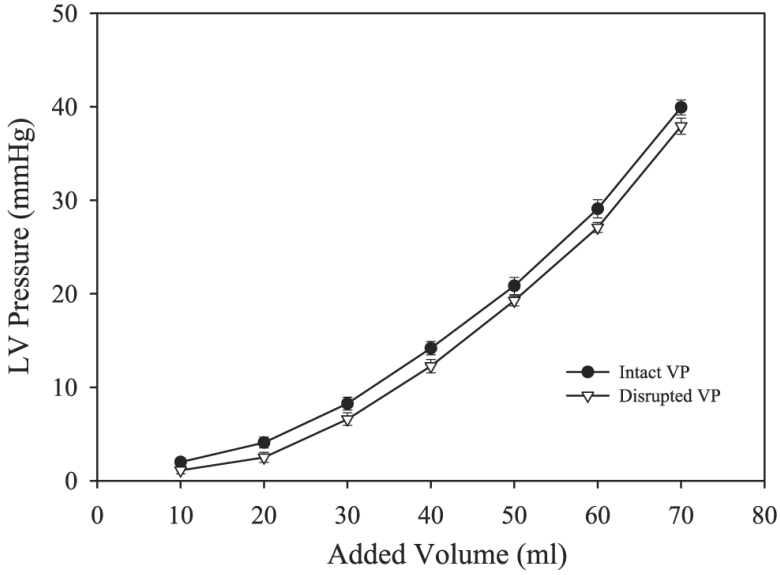

Fig. 6.

Pressure-volume relationship of the LV before and after VP disruption. Disruption of the VP caused a highly significant shift in the entire pressure-volume relationship ($P < 0.05$ by paired *t*-test, $n = 4$).

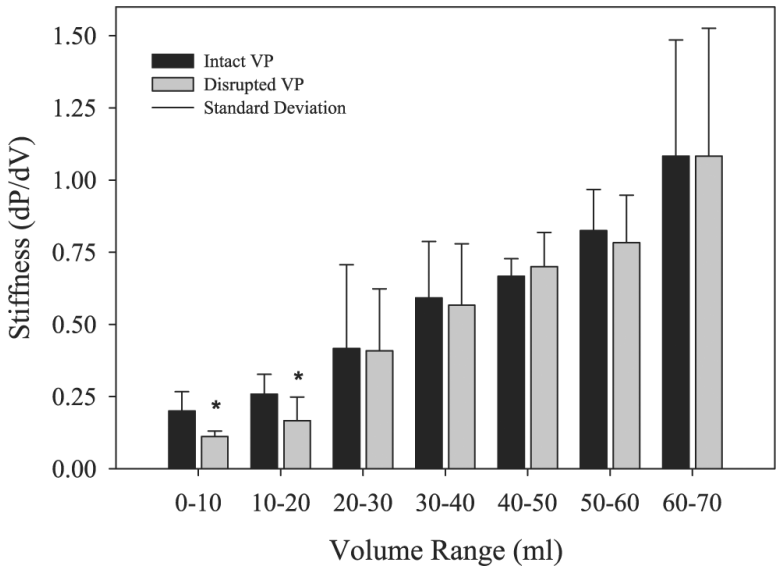

Fig. 7.

LV passive stiffness [change in pressure over volume (dP/dV)] before (intact VP) and after VP disruption. VP disruption significantly reduced LV stiffness at lower volumes, as indicated by the asterisks (0–20 ml, $P < 0.05$), but not in higher volumes (20–70 ml, $P < 0.05$). This suggests that the mechanical effect of VP disruption is primarily due to disruption of the elastin elements of the VP and that other elements remain viable at the higher ranges measured in this study.

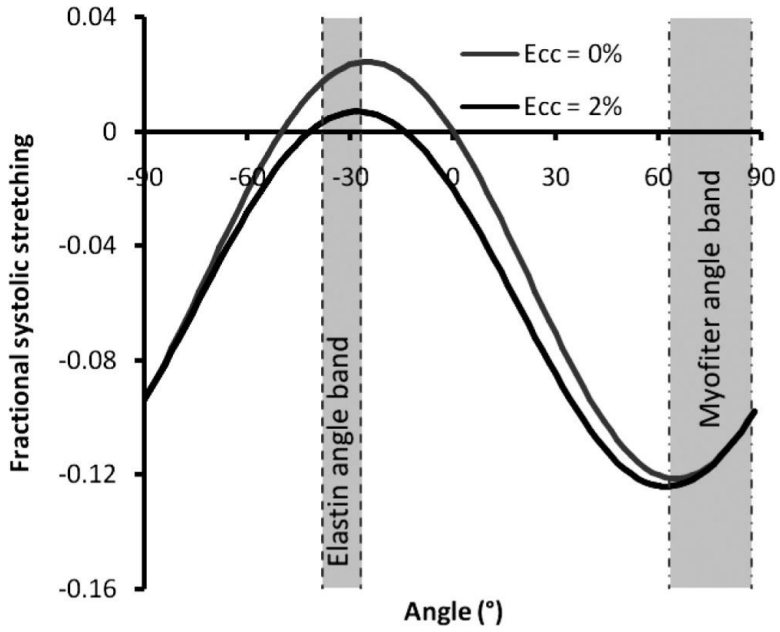

Fig. 8.

Elastin fiber length change during systole versus fiber angle. Two estimates are shown for no appreciable circumferential shortening (E_{cc})on the epicardial surface or 2% E_{cc}. The range of measured elastin fiber angles fell in the region where stretching occurred during systole, whereas the range of measured myofiber angles resulted in the expected 10% shortening. Stretching of elastin fibers is an effective way to store mechanical energy to aid in LV relaxation and untwisting at the onset of diastole.

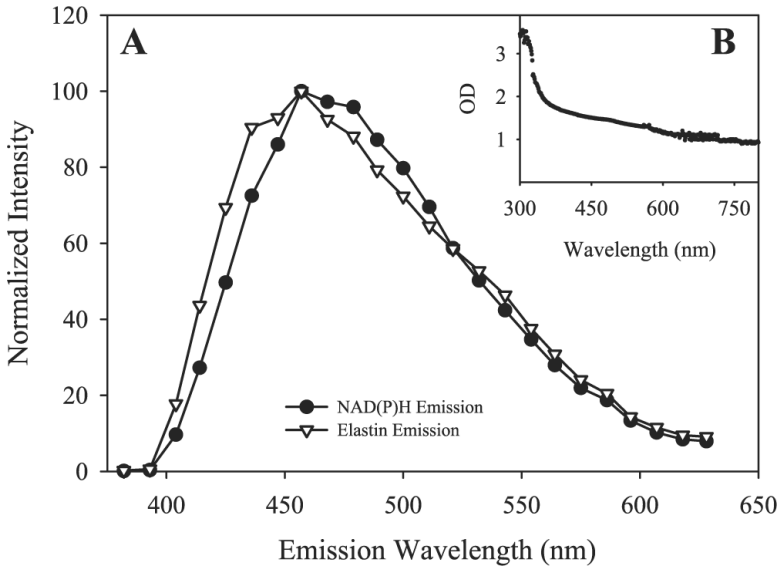

Fig. 9.

A: elastin and NAD(P)H fluorescence collected using the META detector of the Zeiss LSM 510 microscope. The similar absorbance spectra caused difficulty in optically separating the emissions. In *B*, the scattering spectrum of the VP layer, once it had been removed from the myocardium, showed a high degree of scattering from an ~100-μm-thick layer.